THE AMERICAN SOCIETY OF MECHANICAL ENGINEERS
345 E. 47 St., New York, N.Y. 10017

89-GT-188

Impingement/Effusion Cooling: The Influence of the Number of Impingement Holes and Pressure Loss on the Heat Transfer Coefficient

A. M. AL DABAGH, G. E. ANDREWS, R. A. A. ABDUL HUSAIN, C. I. HUSAIN, A. NAZARI and J. WU
Department of Fuel and Energy
The University of Leeds
Leeds, LS2.9JT, U.K.

ABSTRACT

Measurements of the overall heat transfer coefficient within an impingement/effusion cooled wall are presented. The FLUENT CFD computer code has been applied to the internal aerodynamics to demonstrate the importance of the internal recirculation in the impingement gap. This generates a convective heat transfer to the impingement jet and measurements of this heat transfer plate coefficient are presented that show it to be approximately a half of the impingement/effusion heat transfer coefficient. The influence of the relative pressure loss or X/D between the impingement and effusion was investigated, for an effusion X/D of 4.67 and a Z of 8 mm, and shown to be only significant at high G where a reduction in h of 20% occurred. Increasing the number of holes, N, in the impingement/effusion array at a constant Z of 8 mm reduced h by 20%, mainly due to the higher Z/D for the smaller holes at high N. Reduced numbers of impingement holes relative to the effusion holes, in a ratio of 1 to 4, were shown to have a small influence on h with a maximum reduction in h of 20% at high G and a negligible effect at low G.

NOMENCLATURE

A	Total hole approach surface area per hole, m^2. ($A = A^2 - \pi/4\ D^2$).
A_h	Hole internal surface area per hole, m^2 ($A_h = \pi DL$).
A_e	Total effusion hole flow area per hole.
A_i	Total impingement hole flow area per hole
C_p	Specific heat of the wall material.
D	Hole internal diameter, m.
G	Coolant mass flow per unit wall area, kg/sm^2.
h	Surface averaged convective heat transfer coefficient based on the surface area per hole, A, W/m^2K.
k	Thermal conductivity of the coolant, W/mK.
L	Hole length, m.
m	Mass of the test plate heat transfer section, kg.
N	Number of holes per unit surface area, m^{-2}.
Nu	Nusselt number based on h and the impingement hole diameter D, hD/k.
Pr	Prandtl number.
Re	Hole Reynolds number based on the impingement hole diameter D and the coolant velocity in the hole.
T_c	Coolant temperature, K.
T_g	Hot gas temperature, K.
T_I	Impingement jet wall temperature, K.
T_m	Mean wall temperature in central 76 mm of the 152 mm test wall.
T_w	Local wall temperature, K.
T_{wi}	Initial local wall temperature, K.
τ	Time constant, Eq. 6.
X	Hole pitch, m.
Z	Impingement gap, m.

INTRODUCTION

Impingement/effusion cooling of gas turbine combustor and turbine blade walls offers very efficient cooling with minimal coolant mass flow. The double skin wall design is easily manufactured using conventional techniques and thermal stresses

Presented at the Gas Turbine and Aeroengine Congress and Exposition—June 4-8, 1989—Toronto, Ontario, Canada
This paper has been accepted for publication in the Transactions of the ASME
Discussion of it will be accepted at ASME Headquarters until September 30, 1989

are reduced by the double skin design. This allows the outer impingement jet wall to operate at a lower temperature to the inner effusion jet wall. The presence of the effusion holes gives additional heat transfer at the effusion hole inlet and within the short hole (Andrews et al. 1986, 1987). The overall heat transfer coefficient is thus usually higher for impingement/effusion than it is for impingement alone. Hollworth et al. (1980, 1981) for an X/D of 10 and effusion/impingement jet area ratio of 3.07 found an increase of 30% due to the addition of effusion holes offset from the impingement holes. Andrews et al. (1988) found similar increases with values of 30% for an X/D of 10 with an effusion/impingement jet area ratio of 5.6 and 45% for an area ratio of 2.4.

The objective of the present work was to extend the range of impingement/effusion geometries for which overall heat transfer data is available. The influence of the number of holes, N, the relative number of impingement/effusion holes and the area ratio between the impingement and effusion holes were investigated to determine their relative importance. Andrews et al. (1985a) showed that impingement and impingement/effusion heat transfer gave rise to convective heat transfer from the target or effusion wall to the impingement jet wall. This indicated that there was recirculation within the impingement gap and this was investigated using an isothermal model and the FLUENT CFD computer code (Creare, 1985). Heat transfer data is also presented for one geometry for the recirculated convective heat transfer to the impingement jet plate.

Andrews et al. (1988) showed that the dominant heat transfer mode in impingement/effusion internal wall heat transfer was that due to the impingement jets. Far more heat transfer data exists for impingement heat transfer than for the combined impingement/effusion heat transfer. There have been many investigations of impingement heat transfer for multijet arrays, with much of the work aimed at gas turbine cooling applications (Tabakoff and Clevenger, 1972; Kercher and Tabakoff, 1970; Florschuetz et al. 1981; Hollworth and Berry, 1978; Andrews and Hussain, 1984a, b, 1986, 1987, and Andrews et al. 1987b). In the present work the pressure loss of the impingement wall was important and this is determined by the X/D (Andrews and Hussain, 1984a, b). Few general heat transfer correlations exist for impingement heat transfer which include the influence of the main variables, X, D, Z, N and G, over a practical range of values. For a range of X/D from 1.9 to 21.5, Z/D from 0.5 to 35, N from 1,000 - 10,000 m^{-2}, G from 0.1 to 2 kg/sm^2 and Re from 300 to 50,000, Andrews and Hussain (1984a, b) and Andrews et al. (1985d, 1987b) have established the correlation in Eq. 1, which has been shown to be in reasonable agreement with the data of other workers.

$$\frac{Nu}{Pr^{0.33}} = 1.05\ Re^{0.72} \left(\frac{X}{D}\right)^{-0.72} \left(\frac{Z}{D}\right)^{-0.14} D^{0.28} \qquad (1)$$

which in terms of h and G for air for a typical Z/D of 4.5 reduces to Eq. 2.

$$h = 61\ (G\ X/D)^{0.72} \qquad (2)$$

Andrews et al. (1985a) showed that for a practical range of Z from 2-12 mm there was little influence of Z on the impingement heat transfer for X/D from 1.9 to 21.5. For this range of Z the correlation in Eqs. 3 and 4 applied.

$$Nu = 0.29 \left(\frac{X}{D}\right)^{-1.08} Re^{0.72} \qquad (3)$$

$$h = 75 \left(\frac{X}{D}\right)^{0.64} G^{0.72} \qquad (4)$$

In the present work a constant Z of 8 mm was used, well inside the above range of Z for which Eqs. 3 and 4 applied.

In association with the present work there has been a parallel programme on the determination of the overall film cooling effectiveness. This was measured by placing the impingement/effusion test geometry in the wall of a duct with a high temperature crossflow. Andrews et al. (1988) showed typical results for impingement/effusion geometries and demonstrated a significant improvement in the cooling effectiveness of effusion film cooling due to the addition of impingement cooling. The present heat transfer coefficient measurements will be used in a heat balance model of the cooling effectiveness data so as to yield film heat transfer coefficients.

IMPINGEMENT/EFFUSION DESIGN

The combustor design requirements are that the bulk of the pressure loss occurs at the impingement plate and the pressure loss across the effusion wall is small, as this ensures good film cooling characteristics (Andrews et al. 1985b). For turbine blades the relative pressure loss between the impingement and effusion surfaces is more complex than for combustor applications due to large static pressure variations around the blade surfaces. In regions such as the stator vane leading edge, the static pressure at the film cooling hole outlet is very high and a low pressure loss would be necessary at the impingement holes and at the effusion holes. The present work investigates this situation, where the effusion and impingement hole pressure loss are low. Further data is also presented for the situation of a high impingement wall pressure loss with low effusion wall pressure loss. The influence of the number of holes per unit surface area was investigated and the range of geometries is given in Table 1.

In the present work, square arrays of impingement/effusion holes were used with equal numbers of holes offset half a pitch relative to each plate so that an impingement jet was located on the centre of each four effusion holes. All the impingement air was discharged through the effusion holes and

TABLE 1 EXPERIMENTAL IMPINGEMENT/EFFUSION CONFIGURATIONS

Configuration No.	1	2	3	4	5
A_e/A_i	1	1	5.6	1	5.3
Z/D_i	0.5-5	1.0	5.8	6.1	2.8
Impingement Wall					
N m^{-2}	4306	4306	4306	26910	1076
X mm	15.2	15.2	15.2	6.1	30.4
D_i mm	3.24	8.2	1.38	1.32	2.86
X/D	4.7	1.8	11.0	4.7	10.6
152 mm square hole array	10x10	25x25	10x10	25x25	5x5
Effusion Wall					
N m^{-2}	4306	4306	4306	26910	4306
X mm	15.2	15.2	15.2	6.1	15.2
D_e mm	3.27	8.2	3.27	1.32	3.27
X/D_e	4.7	1.8	4.7	4.7	4.7

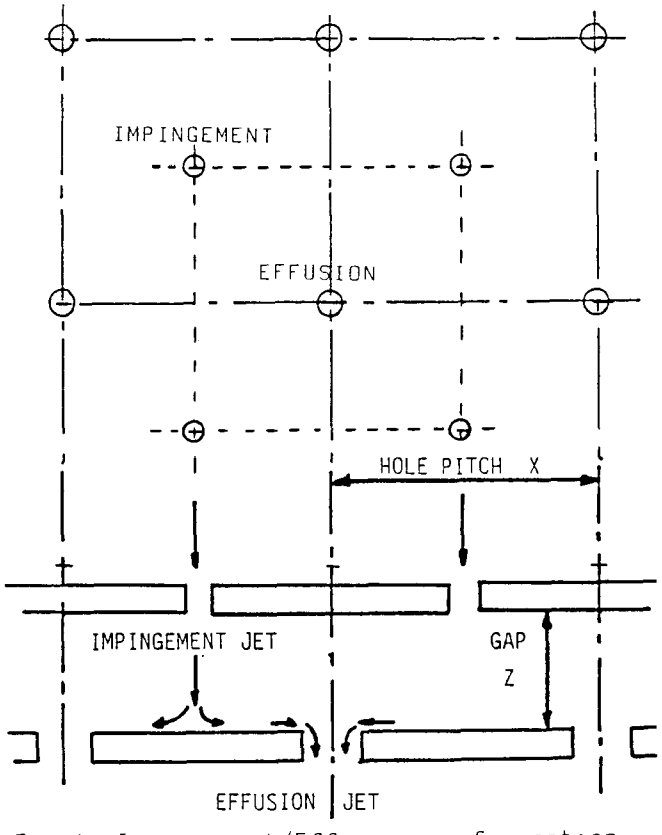

Fig.1 Impingement/Effusion configuration

hence there was no net crossflow in the impingement gap. This test configuration is shown in Fig. 1. For geometries with the main pressure loss at the impingement wall the hole sizes are small and the manufacturing costs relatively high and a minimum number of holes should be used. Effusion film cooling requires a large number

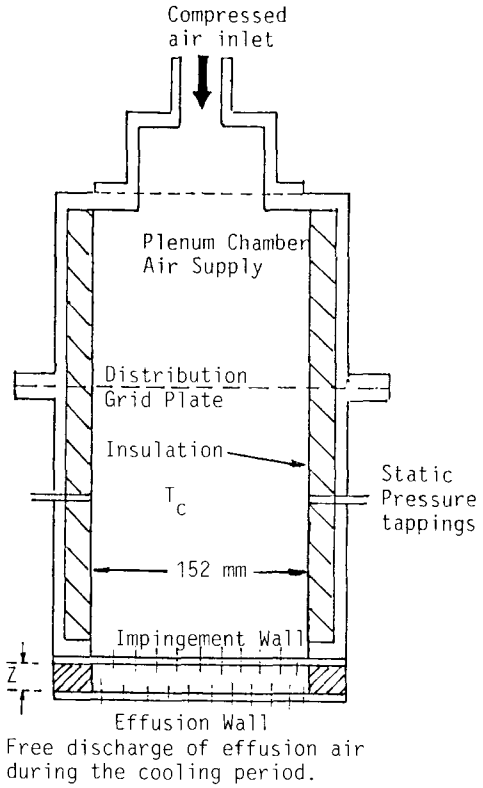

Fig.2 Experimental equipment.

of holes, N, for optimum film cooling effectiveness. Andrews et al. (1987b) showed that for impingement heat transfer N could be varied over a wide range without any major reduction in the heat transfer. Thus, there may be no requirement to have equal numbers of impingement and effusion holes and the variation of their ratio forms part of the present investigations using the geometries detailed in Table 1. Hollworth et al. (1980,1981) used one impingement hole for every four effusion holes and their data was very similar to that of Andrews et al. (1988) for equal numbers of holes.

EXPERIMENTAL TECHNIQUES

The experimental equipment is shown in Fig. 2. A 152 mm square Nimonic 75 test wall was used with a PTFE (Teflon) separation flange forming the impingement gap, which also minimised thermal conduction between the the impingement and effusion test geometries. A range of impingement gap flanges was used to achieve different impingement gap (Z) to hole diameter (D) ratios, Z/D. The impingement/effusion geometry and PTFE separation gaps were all bolted to an internally insulated air supply plenum chamber. Each test plate, both impingement and effusion, was instrumented with at least five Type K mineral insulated grounded junction thermocouples, vacuum brazed to the exit side of the test plates on the centreline of the plate midway between the holes. In addition, the effusion test plate had thermocouples brazed to the feed side of the plate to investigate temperature

gradients. There was no significant difference in the temperature across the effusion plate metal thickness. Previous work using steady state heat transfer techniques showed that temperature gradients, both axially between the jets and through the wall thickness, were less than 2% of the mean wall temperature (Andrews and Hussain, 1984b). This was in agreement with the findings of the more complex film cooling situation where even at high temperatures the test plate was at a uniform temperature with maximum temperature differences of less than 3% of the mean temperature (Andrews et al. 1985c). The test plate centreline thermocouples were used for the heat transfer measurements, rather than the mean plate temperature as this avoided any slight edge effects. By comparing h determined from different thermocouples, the experimental uncertainty was evaluated.

The heat transfer coefficient was determined by using a transient cooling technique. This was the same as that used for single wall effusion cooling short hole heat transfer (Andrews et al. 1986a, 1987a). The impingement/effusion test wall was heated in the absence of any coolant air flow by placing the wall and plenum chamber assembly on an insulated uniform heat flux electrical mat heater. Prior to heating the wall, the air flow controls were set to give the desired air flow by opening a single valve. The test wall was heated to approximately 80°C and then rapidly hoisted free of the heater and the coolant flow established. The test plate was then cooled by the air flow and the temperatures of all the thermocouples were recorded as a function of time using a thirty-two channel data acquisition system interfaced to a microcomputer.

The transient cooling of the impingement/effusion assembly is governed by the classical first order differential equation with a solution for a step change in heat input that gives an exponential fall in temperature with time. These equations are valid provided the wall was at a uniform temperature. For convective heat transfer to a slab, a uniform wall temperature is achieved if the Biot number is low. For the present work, the Biot number was always less than 0.2 and temperature differences of less than 10% of the mean would be expected from classical heat conduction analysis. For most of the test conditions, the Biot number was less than 0.1 and temperature gradients less than 5% of the mean would be expected. The experimental measurements of maximum temperature gradients, discussed above, were all less than 5%. Successive temperature data points were used to determine the time constant, τ, from Equations 5 and 6. Each pair of successive temperatures were used to calculate $\Delta T_w / \Delta t$ and this was associated with the mean of the two

$$Tw = T_c - \tau \frac{\Delta T_w}{\Delta t} \qquad (5)$$

$$\tau = \frac{m\, c_p}{h\, A} \qquad (6)$$

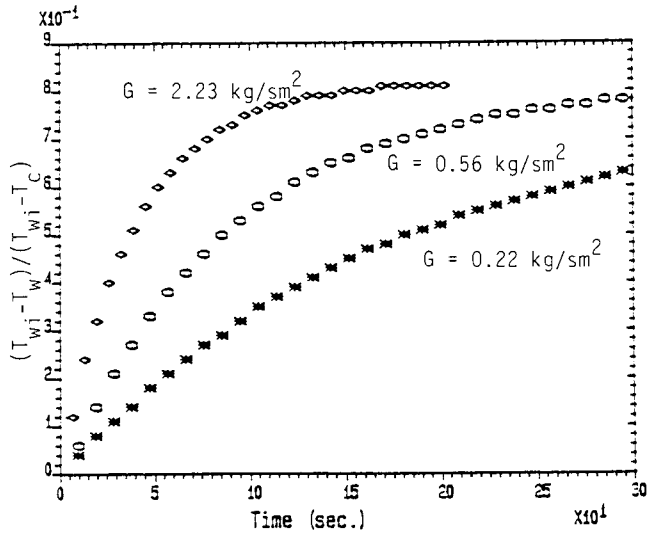

Fig.3 Transient cooling response of the effusion wall for configuration No.1, X/D=4.7, Z=8mm, for three flow rates G of 0.22, 0.56 and 2.23 kg/sm²

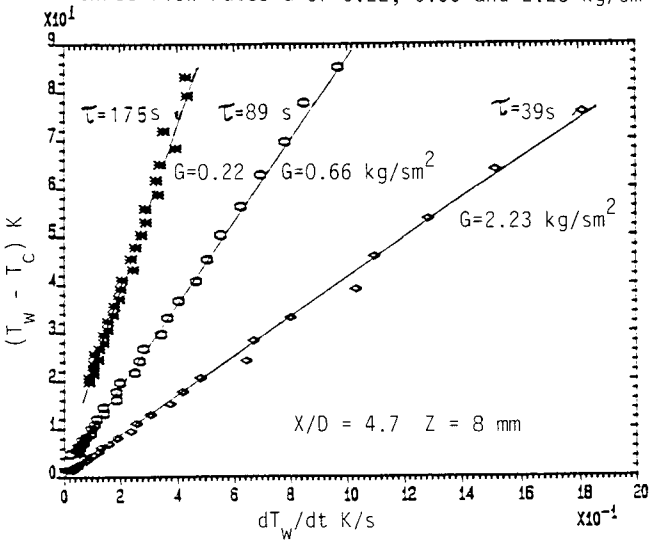

Fig.4 Determination of the time constant from the transient cooling response for configuration 1

temperatures. This mean temperature, T_w, was then plotted against $\Delta T_w / \Delta t$ and a least square fit was made to the data to yield the gradient, which was τ. Equation 6 shows that h may be calculated directly from τ as the other parameters are all known constants for a particular plate material and geometry. This technique was used in the present work to determine the heat transfer coefficient for both the effusion wall and the recirculated heat transfer to the impingement jet wall.

The choice of the dominant heat transfer surface area, A, to use in Eq. 6, is crucial to the establishment of a viable heat transfer correlation. In an impingement/effusion situation, the choice of area is uncertain as the impingement heat transfer acts over the effusion plate surface area, whereas conventionally the effusion plate heat transfer is ascribed to the internal hole surface area, A_h. However, Andrews et

al. (1986,1987a) have shown that the effusion plate cooling was dominated by the hole approach surface heat transfer and that the effusion plate surface area, A, was the most appropriate area to use in the correlation. As this is the same area as used for the impingement heat transfer coefficient, the comparison between impingement, effusion and impingement/effusion systems is easily made.

The heat transfer coefficient was evaluated for each thermocouple on the test walls, so that the variations in h over the test surface could be determined. Typical transient test results for a single thermocouple are shown in Figs. 3 and 4 for a range of G. Other heat losses from the test section, such as convection from the bottom side of the wall, were small and do not influence the transient response as the heat transfer coefficients were much smaller than those being measured. The transient response analysis was confined to the rapid cooling part of the results, where any temperature change due to other lower convective heat transfer events would be negligible. Edge conduction losses were also small during the transient and heat losses were much less of a problem than during steady state heat balance tests. The least squares fit to the data in Fig. 4 gave a maximum uncertainty in an individual measurement of τ and hence in h of $\pm$ 5%. The uniformity of h with axial distance on the centreline of the test wall is shown in Fig. 5 for a range of G. Taking the 95% confidence limits as twice the standard deviation than Fig. 5 shows h to be constant on the test wall centreline to $\pm$ 1% of h at low G and $\pm$ 3% of h at high G. This small deterioration in the confidence limits at high G was due to the small increase in Biot number.

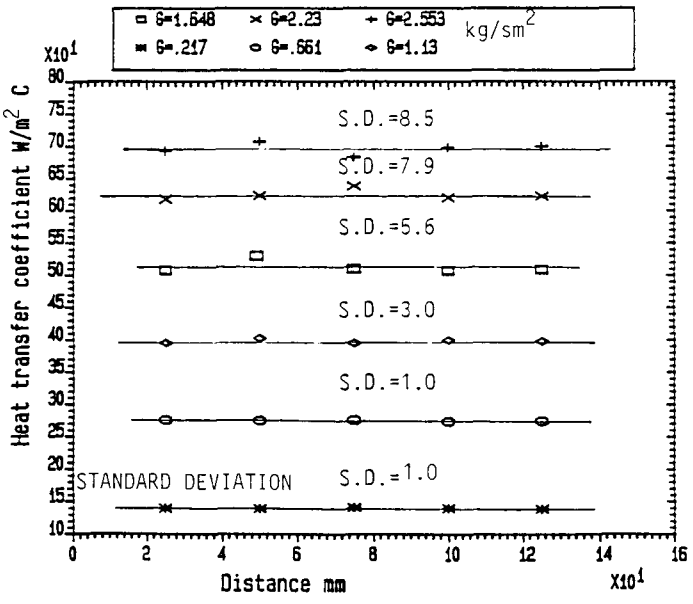

Fig.5 Axial variation of h on the effusion wall for configuration 1, X/D=4.7, Z/D=3, for a range of G from 0.22 - 2.55 kg/sm^2.

AERODYNAMICS IN THE IMPINGEMENT/EFFUSION GAP

The aerodynamics in the gap between the impingement and effusion walls is complex with recirculation between the impingement jets. This was investigated initially in a simplified two dimensional form using both water flow visualisation and the FLUENT CFD code (Creare, 1985). Typical predicted flow

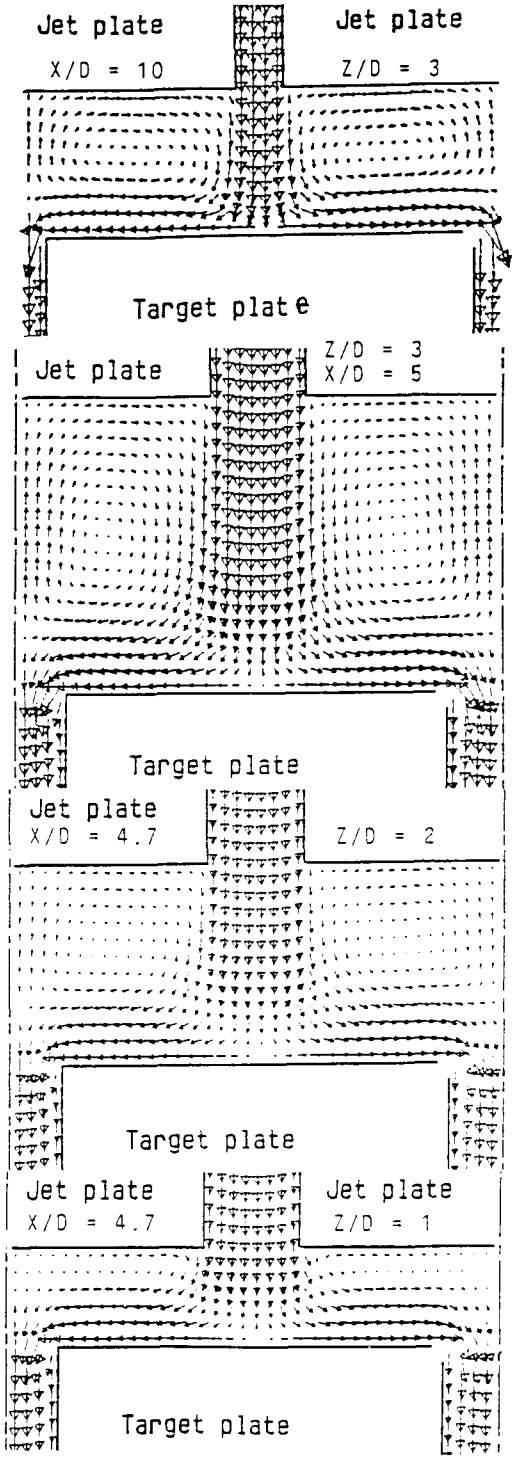

Fig.6 Impingement/Effusion gap aerodynamics predicted using the FLUENT CFD code in 2D (Creare, 1985)

patterns are shown in Fig. 6 for a range of geometries of relevance to the present work. These were very close to the flow visualisation flow patterns. They show that on the centreline between the impingement jets there was a strong reverse flow jet between two counter rotating vortices. In the two dimensional simulation, the reverse flow jet was directly in line with the effusion jet, which would reduce the reverse flow velocity compared with the three dimensional situation of offset impingement and effusion hole centre lines.

Fig. 6 shows that high velocities were induced in opposite directions on the jet and effusion target walls. These wall velocities are shown in Figs. 7 and 8 as a ratio of the inlet jet velocity, for a range of jet velocities for one impingement/effusion configuration. Fig. 7 shows that the peak velocities on the jet plate surface were as high as 25% of those of the jet velocity. This was the main cause of the convective heat transfer to the jet plate from the effusion plate that is detailed later.

Fig. 7 shows the velocity variation along the effusion plate surface as a ratio of the impingement jet velocity. This shows that at the edge of the effusion hole the velocity was 30% higher than the jet velocity. This was the source of the enhanced heat transfer due to the presence of the effusion holes. Andrews et al. (1988) showed that the impingement/effusion heat transfer was mainly due to the addition of the impingement and effusion heat transfer. However, there was a 15-20% over prediction of the measured impingement/effusion heat transfer co-efficient using the summation of the separately measured impingement and effusion heat transfer coefficients. This over-prediction was considered to be partially due to aerodynamic interaction effects in the combined geometry, as shown in Fig. 6.

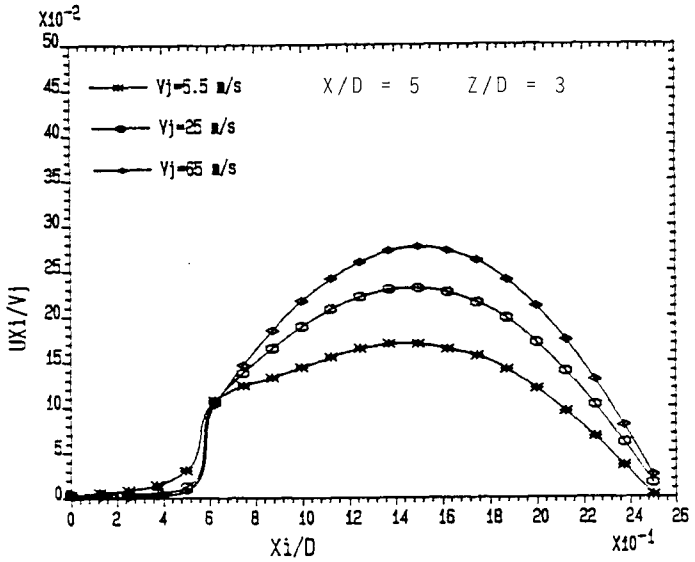

Fig.7 FLUENT 2D computations of the horizontal velocity distribution on the impingement wall due to recirculation in the gap. Horizontal velocity expressed as a ratio to the impingement jet velocity.

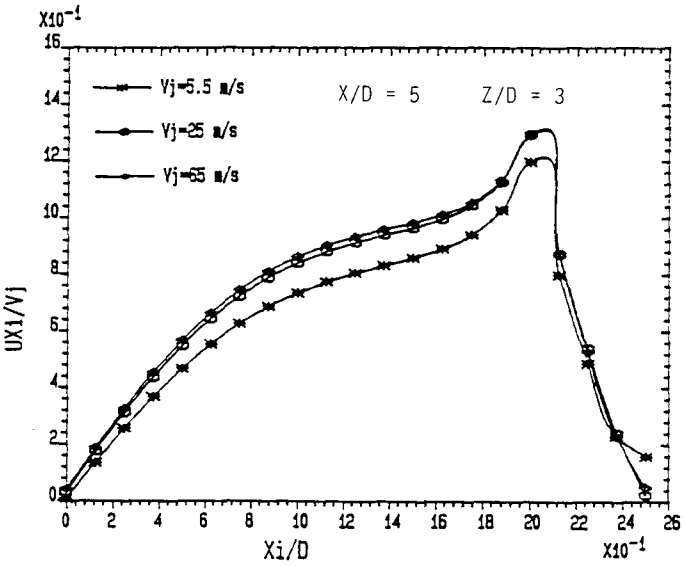

Fig.8 Horizontal surface velocity distribution on the effusion wall gap side, velocities expressed as a ratio to the impingement jet velocity, 2D predictions using the FLUENT CFD code (Creare).

IMPINGEMENT JET WALL HEAT TRANSFER

The heating of the impingement jet wall due to the recirculation of heat by the aerodynamics shown in Fig. 6 was first measured experimentally by Andrews et al (1985a). The heating of the impingement jet plate was expressed by the dimensionless temperature T_z, defined by Eq. 7

$$T_z = \frac{T_I - T_c}{T_m - T_c} \qquad (7)$$

A comparison of the steady state T_z results for impingement/effusion cooling with those for impingement only is made in Fig. 9. At low coolant flow rates, G, the impingement jet plate was heated quite appreciably. This would transfer heat to the impingement air raising its temperature above the supply

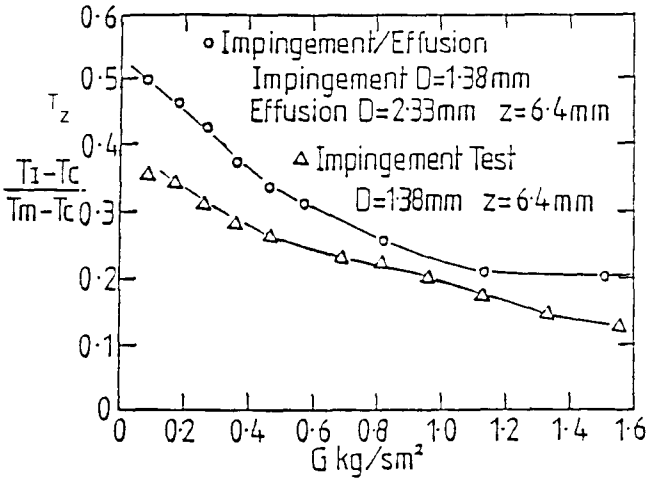

FIG. 9 T_z v. G for impingement/effusion and impingement alone.

coolant temperature, T_c. The impingement results were obtained on the present equipment during steady state operation. Reliable steady state results could not be established with impingement/effusion cooling due to the flow of coolant through the heater. The results in Fig. 9 were obtained from high temperature tests with the impingement/effusion wall mounted flush in the wall of a 76 x 152 mm duct with high velocity propane combustion products at 750K as the heat source. The effusion jets provided film cooling and the results were presented by Andrews et al. (1988). Considering the major differences between the two test facilities, the agreement in the values of T_z in Fig. 9 is quite good. The higher values for impingement/effusion may be due to the acceleration of the reverse flow jet, shown in Fig. 6, by the heating received during the impingement heat transfer.

Values of T_z as a function of the impingement gap, Z, for a coolant flow rate, G, of 0.45 kg/sm^2 are shown in Fig. 10 for a range of impingement jet diameters. At low Z values the inter wall heating was very significant. In this region the Z/D was less than unity and the flow aerodynamics did not exhibit recirculation but high velocity flow from wall to wall across the impingement gap. The transition to this type of flow can be seen for a Z/D of 1 in Fig. 6. At low Z this effect is greater the higher the impingement hole diameter and the smaller the X/D. For larger Z, where the counter rotating vortices shown in Fig. 6 exist, T_z increases with reduced hole size or increased X/D. This was because the reverse flow jet velocity was greater due to the higher impingement jet velocity with consequently greater reverse flow heat transfer.

The transient cooling technique was used to simultaneously determine the impingement jet wall and target effusion wall heat transfer coefficients. The impingement/effusion configuration 1 in Table 1 was used.

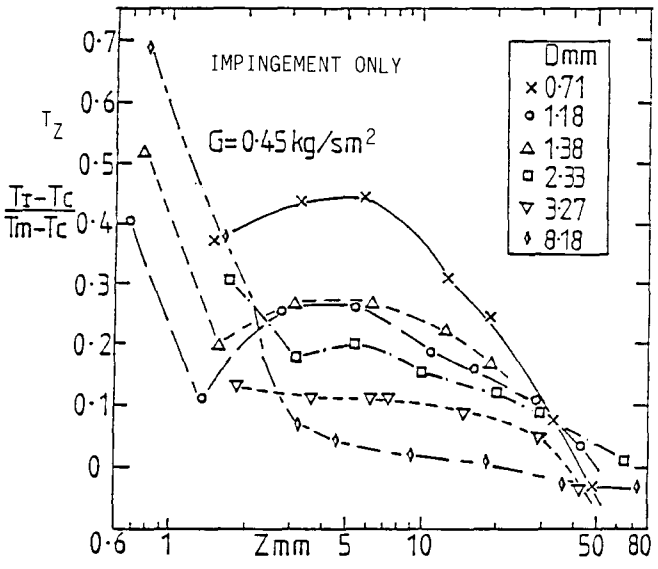

FIG. 10 T_z as a function of Z for G=0.45 Kg/sm^2

This had equal impingement and effusion hole sizes and was designed for a low overall pressure difference application. Fig. 10 showed that the impingement gap was an important parameter in determining the magnitude of T_z. Consequently, the impingement gap was varied for configuration 1 giving a range of Z/D from 0.5-5. The results as $Nu/Pr^{0.33}$ as a function of the impingement jet Re are shown in Figs. 11 and 12 for the effusion and impingement jet walls respectively.

Figure 11 shows that there was a negligible influence of Z/D on the heat transfer to the effusion wall. Z/D cannot influence the heat transfer due to the effusion hole and hence any influence of Z/D must be due to the impingement heat transfer. Andrews et al. (1985d) showed, for the 3.2 mm diameter impingement jet plate of configuration 1 in Table 1, that there was only a small influence of Z/D on the impingement heat transfer over the range of Z/D from 0.5 to 5 for a constant G. The prediction of the aerodynamics in the impingement/effusion gaps using the FLUENT CFD programme showed that the flow along the effusion wall had no strong dependence on Z/D, as shown in Fig. 6. However, the interjet recirculation zone aerodynamics were significantly influenced by Z/D.

Figure 12 shows that Z/D had a strong influence on the heat transfer due to the

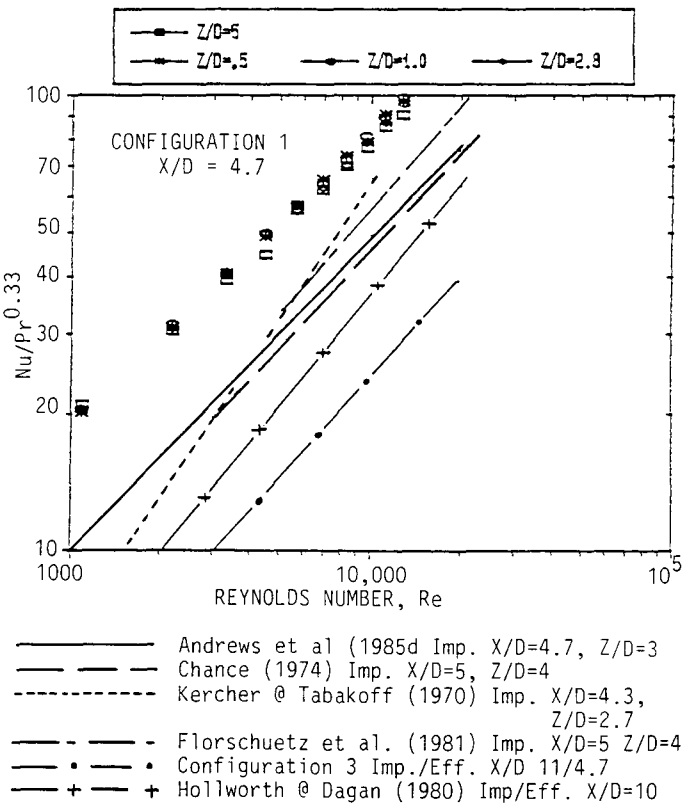

Fig.11 Influence of Re on heat transfer for configuration 1 at various Z/D and configuration 3 at Z=8mm, with a comparison with previous data for similar geometries for impingement and impingement/effusion.

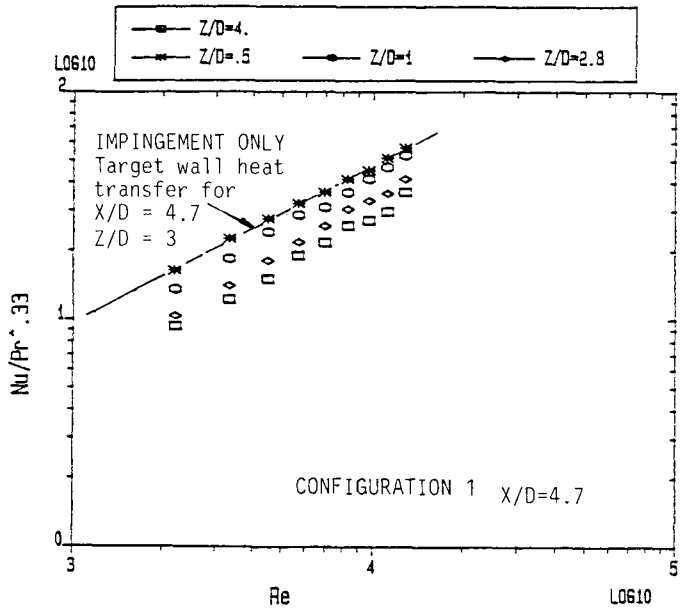

Fig.12 Heat transfer to the impingement wall due to recirculation within the impingement gap.

internal flow recirculation from the effusion wall to the impingement jet wall, as was found for T_z in Fig. 10. Heat transfer increased as Z/D was reduced due to the more compact recirculation and the full gap width flow at Z/D < 1. Comparison of the heat transfer data in Figs. 11 and 12 show that at low Z/D the impingement jet plate heat transfer was approximately half that of the combined impingement/effusion heat transfer. However, if the impingement jet plate heat transfer data is compared with the impingement target plate data of Andrews et al. (1984) for the 3.2 mm impingement jet array, then these two heat transfer results are quite similar as shown in Fig. 12. This indicates that this reverse flow heat transfer was of a very significant magnitude and was an important feature of both impingement and impingement/effusion cooling systems.

COMPARISON WITH PREVIOUS IMPINGEMENT HEAT TRANSFER RESULTS

The present results are compared with a range of previous heat transfer data in Fig. 11. For impingement/effusion heat transfer, the results for configuration 3 in Table 1 (Andrews et al. 1988) are compared with those of Hollworth and Dagan (1980) for an X/D of 10. They used a steady state heat balance technique with a very low N and large D. In spite of these differences there was reasonable agreement with the present results.

For impingement heat transfer only, the steady state impingement heat transfer results for configuration 1 with an X/D of 4.7 and a Z/D of 4 (Andrews and Hussain, 1984b) are shown in Fig. 11. These results are in excellent agreement with those of Chance (1974) for an X/D of 5.3 and a Z/D of 4. They are also in reasonable agreement with the results of Florschuetz et al. (1981)

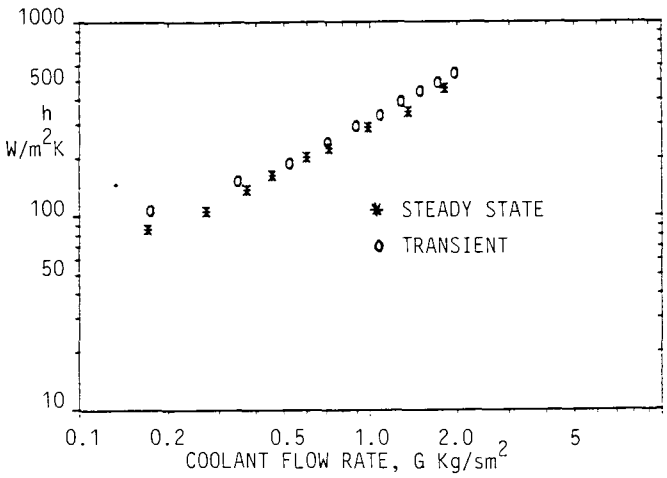

Fig.13 Comparison of steady state and transient techniques for the determination of h for impingement heat transfer with X/D=6.8 Z=8mm.

for an X/D of 5 and Z/D of 3, and with the results of Kercher and Tabakoff (1970) for an X/D of 4.3 and a Z/D of 2.7.

The present transient techniques for determining h have also been applied to impingement heat transfer alone. The results are compared in Fig. 13 with the steady state results of Andrews et al. (1985a) for N=4306 m^{-2} and an X/D of 6.83 (D=2.33 mm). The agreement between the two quite different techniques for determining h was good, with a maximum difference of 20% between the results for the same G. The transient results were slightly higher than for the steady state results and this may have been due to the lower influence of heat losses in the transient tests. These results indicate that valid comparisons may be made between the present impingement/effusion transient results in Fig. 14, and the previously published steady state results.

LOW PRESSURE LOSS IMPINGEMENT/EFFUSION HEAT TRANSFER

For some turbine blade cooling applications a low overall wall pressure loss is required across the impingement/effusion wall. The pressure loss is directly controlled, at a fixed flow rate G, by the hole pitch to diameter ratio as shown by Eq. 8 (Andrews et al. 1985d). Equation 8 shows that a low pressure loss

$$\frac{X}{D} = \text{const} \frac{(\Delta P/P)^{0.25}}{G^{0.5}} \qquad (8)$$

requires a small value of X/D. In the present work values of X/D of 4.7 and 1.8 were used, which are typical of the X/D used in some turbine blade cooling designs. Previous work for combustion chamber applications (Andrews et al. 1988) used a high pressure loss impingement jet wall (X/D=11) with low pressure loss effusion walls (X/D=4.7) and these results will be used for comparison. The same hole size and X/D was used for the impingement and effusion

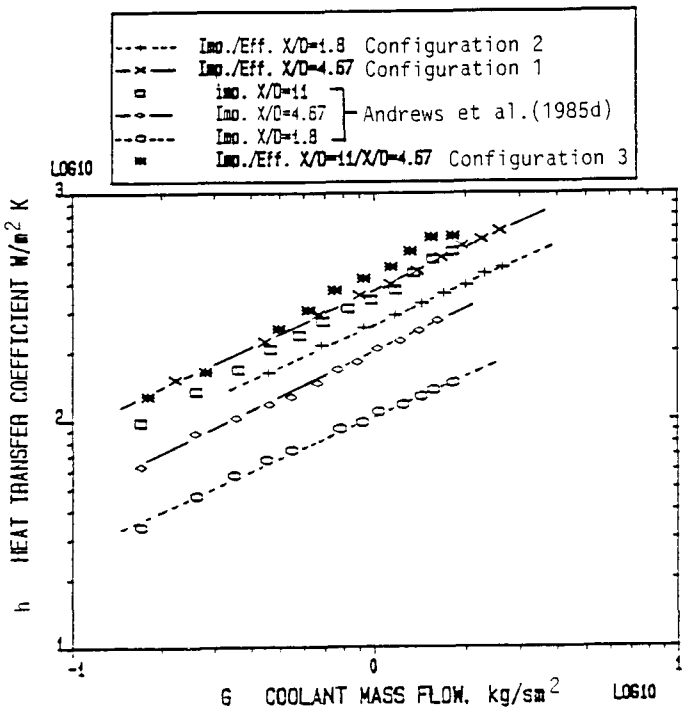

Fig.14 Heat transfer coefficient as a function of G for impingement alone and impingement/effusion at Z/D=3, with different X/D.

walls to achieve the desired low overall pressure loss. The design details of all these three configurations are given in Table 1.

The influence of Z/D for configuration 1 was shown above to be small for a wide range of Z/D. A small Z/D of unity was used for configuration 2, which gave a practical impingement gap size for the relatively large hole diameter. The 8 mm gap used for configuration 3 in Table 1, resulted in a Z/D of 5.8 compared with 1.0 for configuration 2 for the same gap width. Fig. 11 shows that the effusion wall heat transfer was insensitive to Z/D over this range and hence a valid comparison between the present and previous work at different Z/D can be made.

The results for impingement/effusion configurations 1, 2 and 3 are shown as the heat transfer coefficient as a function of coolant flow rate, G, in Fig. 14. The heat transfer coefficient data for the impingement jet wall are also included for comparison in Fig. 14, taken from the work of Andrews et al. (1985d), which used a steady state heat balance technique to determine h.

Fig. 13 shows that for impingement/effusion heat transfer with the same effusion wall X/D of 4.7, the effect of decreasing the impingement X/D from 11 to 4.7 was to decrease h by approximately 20% at high G. However, at low G the influence of impingement X/D was negligible. This effect was much less than the equivalent difference in the two impingement heat transfer coefficients, which Fig. 13 shows to have decreased by approximately 40% at all G. This shows that the influence of the effusion wall jets on the increase in the impingement heat transfer was greater for low X/D impingement geometries than for the high pressure loss and high X/D geometries. The increase in the heat transfer coefficient due to the addition of the effusion holes was a factor of 1.8 for an impingement X/D of 4.7 compared with 1.3 for an X/D of 11 (Andrews et al., 1988). Hollworth and Dagan (1980) also found an increase in heat transfer of 1.3 for an X/D of 11.

For configuration 2 with an X/D of 1.8 at both the impingement and effusion walls, there was a decrease in h compared with configuration 1 of approximately 30% compared with a difference of 50% in the two impingement heat transfer coefficients. However, the combined impingement/effusion heat transfer coefficients for an X/D of 1.8 was approximately 25% higher than the impingement h for an X/D of 4.7 he relatively large reduction in h , for impingement/effusion heat transfer with an X/D 1.8 compared with that for an X/D of 4.7, was contributed to by a reduction in the effusion wall h as well as the impingement wall h. Hence, where possible the X/D should be at least 4.7 for both the impingement and effusion walls if the heat transfer coefficient is to be maximised for a given G for a low overall pressure loss.

The increase in the heat transfer coefficient due to the addition of the effusion holes was a factor of 2.3 for an X/D=1.8 compared with 1.8 for an X/D of 4.7 and 1.3 for configuration 3 with an impingement X/D of 11. The reason for the greater relative influence of the effusion wall at low X/D was the additive effect of the impingement and the effusion hole entry heat transfer. Reducing the impingement X/D at constant effusion X/D simply reduces the proportion of the overall heat transfer due to impingement, as the effusion hole entry heat transfer remained unchanged.

For an X/D of 4.7, configuration 1, the value of h at a G of 1 kg/sm^2 was 200 w/m^{2}k for the impingement jets (Andrews et al. 1985d) and also 200 w/m^{2}k for the effusion wall (Andrews et al. 1987a). With no interaction between the two heat transfer modes, the combined heat transfer should be 400 compared with the measured 360 w/m^{2}k. This was only a 10% reduction in heat transfer due to interaction effects compared with 19% for an impingement X/D of 11 (Andrews et al. 1988). For the X/D of 1.8 configuration, the combined impingement and effusion heat transfer coefficient was the same as the present measured impingement/effusion heat transfer and there was thus no significant interaction. The reason for this was the more rapid decay of the impingement jet velocities on the surface of the effusion wall for low X/D. For an X/D of 11 but the same X as the lower X/D results, this surface velocity was high and would dominate the effusion hole entry velocities. Thus the enhancement of the velocities at the effusion hole lip, as shown for an X/D of 5 in Fig. 8, was considerably reduced for an X/D of 11.

INFLUENCE OF THE NUMBER OF HOLES

Andrews et al. (1987b) showed that for the impingement heat transfer there was little major influence of the number of holes per unit surface area, N, over a wide range of N. Reduced heat transfer was found at very low values of N and very high values. This was due to lack of adequate surface coverage of the enhanced heat transfer regions at low N and crossflow effects at high N. The aim of the present work was to investigate whether there was any advantage in using a high N for impingement/effusion cooling.

Configurations 1-3 in Table 1 were for an N of 4306 m^{-2} and for an X/D of 4.7, these results were compared at a Z of 8 mm with those for an N of 26910/m^2, configuration 4. This comparison is shown in Fig. 15 as h v. G which shows that there was a small reduction in the heat transfer coefficient with increased N in the impingement/effusion array and hence that there was no advantage in using the much higher number of holes of configuration 4.

The decrease in heat transfer with the increase in N shown in Fig. 15 was approximately 20% at all G. Part of the reason for this decreased heat transfer was the use of an 8 mm impingement gap for both tests. This involved different Z/D as shown in Table 1, with a Z/D of 2.5 for an N of 4306 m^{-2} and 6.1 for an N of 26910 m^{-2}. The Z/D exponent of 0.14 in Eq. 1 is sufficient to account for the 20% lower heat transfer at the larger Z/D. An impingement gap of approximately 3 mm would be required for the same Z/D as at an N of 4306 m^{-2}. This is feasible for turbine blade applications but too small for large surface area combustor applications.

The results for impingement heat transfer (Andrews et al. 1987b) also showed that there

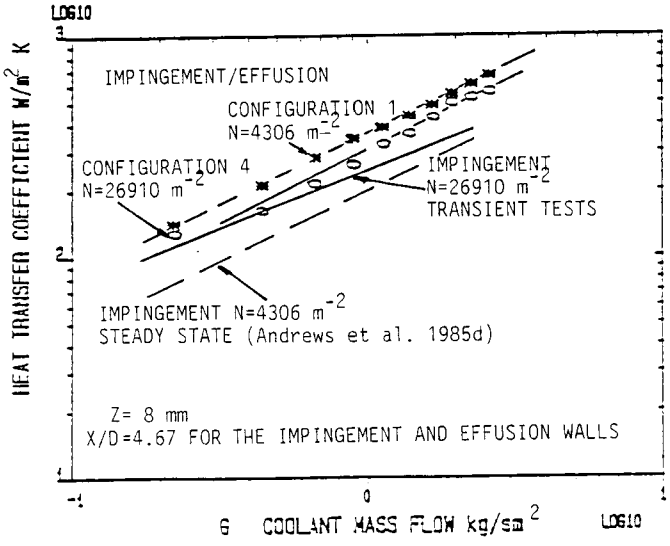

Fig.15 Impingement/effusion and impingement heat transfer coefficients as a function of G for different numbers of holes, N=4306 and 26910 m^{-2}, for an X/D of 4.7 for the impingement and effusion walls

was a deterioration in heat transfer a Z of 10 mm and N of 26910/m^2 compared with an N of 4306/m^2. The reasons for this difference was the influence of crossflow in the impingement gap with impingement cooling alone. Crossflow in the impingement gap decreases the heat transfer and this effect increased with the number of rows of upstream holes and with a decrease in Z/D (Andrews and Hussain, 1986, 1987).

The impingement results in Fig. 13 were obtained for a flow discharge on all edges of the impingement gap and this minimised the impingement crossflow influence, compared with the more usual single sided flow exit. However, in impingement/effusion cooling with equal numbers of impingement and effusion jets there can be no crossflow and hence there should be no deterioration in the impingement heat transfer at any value of N. Under these circumstances, a minimum value of N can be used to minimise manufacturing costs and the only limit is that of adequate surface coverage of the high impingement heat transfer. For this minimum N, a small Z/D should be used to achieve practical impingement gaps.

REDUCED NUMBER OF IMPINGEMENT JETS RELATIVE TO THE EFFUSION JETS

Hollworth and Dagan (1980) have emphasised that design features which maximise the heat transfer of the coolant as it passes through the impingement effusion wall will be different from those that maximise the film cooling effectiveness of the effusion jets. Andrews et al. (1985b,c) have investigated the film cooling performance of some of the present effusion designs. They showed that the film cooling effectiveness and the overall cooling effectiveness increased as the X/D was reduced for a fixed number of holes. This was achieved by increasing the hole diameter which reduced the effusion wall pressure loss. In subsequent unpublished work, the authors have also shown that there was a very strong influence of the number of effusion holes on the film and overall cooling effectiveness. Thus the requirements for optimum effusion cooling in impingement/effusion cooling are different from those for optimum impingement cooling. A major difference is in the influence of the number of holes N.

For optimum effusion film cooling a large N was required, but this was not necessary for the impingement cooling. Also the impingement hole size becomes very small and manufacturing costs increase if a large N is used, together with a high impingement wall pressure loss. Consequently, there are advantages in using different numbers of impingement and effusion holes. Hollworth and Dagan (1980) used one impingement hole for every four effusion holes with both sets of holes of similar diameter. This gave an area ratio of 3.07 between the effusion and impingement jets. Andrews et al. (1988) investigate area ratios of 2.4 and 5.6 using equal numbers of holes but larger effusion

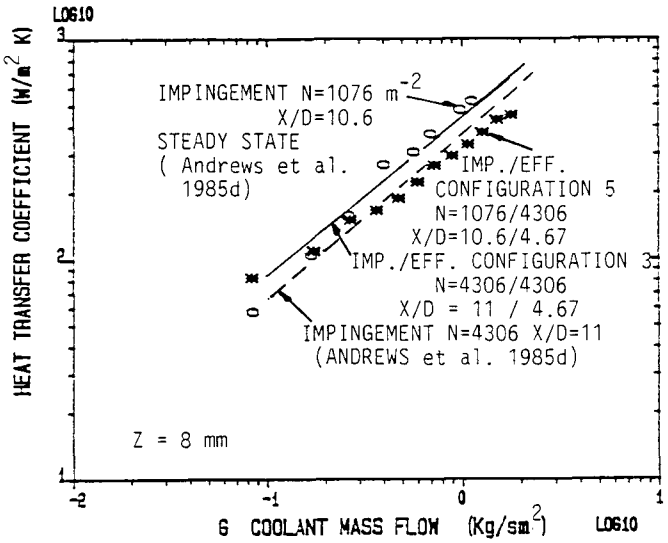

Fig.16 Comparison of h as a function of G for impingement/effusion configurations 3 and 5 with different numbers of impingement holes but the same impingment X/D.

hole diameters. Their results were shown to be in good agreement with those of Hollworth and Dagan (1980) for the same impingement jet X/D.

In the present work the number of impingement jets was reduced and the same effusion wall was used as for the equal number of jets situation. However, the diameter of the impingement jets were increased so that the same area ratio of 5.6 was used for both configurations. One impingement hole was used for four effusion holes and the design, configuration 5, is detailed in Table 1. The heat transfer results are compared with the results for an equal number of holes in Fig. 16, and this also includes the impingement heat transfer results for Andrews et al. (1987b) for the reduced number of impingement jets without any effusion jets. The reduced number of impingement jets has a small influence on the impingement/effusion heat transfer. Fig. 16 shows that at a high G of 1-2 kg/sm^2 the reduction in heat transfer was approximately 20%, but at a low G of below 0.3 kg/sm^2 there was a negligible difference between the results.

It is considered that the decrease in the impingement/effusion heat transfer coefficient at high G, with a reduced number of impingement holes was due to an increase in the interaction between the two heat transfer modes. The impingement jets will set up a very similar double vortex aerodynamics to those shown in Fig. 6, but the effusion jets will no longer be in the plane of the reverse flow jet. They will be exposed to a potentially high velocity crossflow across the hole entrance. There will thus be a much reduced enhanced heat transfer due to the flow acceleration into the hole. The combined heat transfer will thus be dominated by the impingement jets with little additive heat transfer.

Comparison of the impingement/effusion results with those for impingement alone in Fig. 16 shows a deterioration in heat transfer with the addition of effusion jets, of approximately 30% at high G (0.3 kg/sm^2), but negligible at low G (0.3 kg/sm^2). This was possible due to the reduction in impingement heat transfer due to the removal of impingement mass flow in the high velocity near impingement jet region with a consequent reduction in surface velocities and gap recirculation rates. However, the addition of the impingement heat transfer to the effusion wall resulted in a 65% increase in the heat transfer coefficient, as shown in Fig. 16. Thus, even though the interaction between the impingement and effusion aerodynamics resulted in a deterioration in both modes of heat transfer, the combined effect was still a substantial increase on that for the effusion wall alone.

CONCLUSIONS

1. The internal aerodynamics in the gap between the impingement and effusion walls are complex and are dominated by the counter rotating vortices between the impingement jets, with a reverse flowing jet in-line with the effusion hole. This causes significant heat transfer to the impingement jet plate.

2. For equal numbers of impingement and effusion holes the interaction between the two heat transfer components is small and the effusion wall gives an additive heat transfer to the impingement jets and the overall heat transfer for impingement/effusion is much higher than for impingement alone. However, if the number of impingement jets is lower than the number of effusion jets then the interaction between the two heat transfer components is larger and little additional heat transfer due to the effusion holes then occurs.

3. The area ratio between the effusion and impingement holes influences the heat transfer coefficient with larger values for large area ratios. However, the effect is not large and systems with equal hole size and equal numbers of holes have a high heat transfer coefficient with less impingement and effusion heat transfer interaction.

4. Increasing the number of impingement and effusion holes at constant Z caused a small decrease in the impingement/effusion wall heat transfer coefficient, due to the increased Z/D at constant N and X/D.

ACKNOWLEDGEMENTS

We would like to thank the U.K. Science and Engineering Research Council for a research grant, GR/D/53029, in support of this work. Some of the test geometries were manufactured by GEC/Ruston Gas Turbines and we would like to thank M.F. Cannon for technical advice. A.M. Al Dabagh and R.A.A. Abdul Husain received research scholarships from the Iraqi Government.

REFERENCES

Andrews, G.E. and Hussain, C.I., 1984a, "Impingement Cooling of Gas Turbine Components", 1983 Tokyo International Gas Turbine Conference, pp.67-74, and High Temperature Technology, Vol. 2, pp.99-106.

Andrews, G.E. and Hussain, C.I., 1984b, "Full Coverage Impingement Heat Transfer: The Influence of Impingement Jet Size", 1st U.K. National Heat Transfer Conference, I.Chem.E. Symposium Series No. 86, Vol. 2, pp.115-1124.

Andrews, G.E. and Hussain, C.I., 1986, "Full Coverage Impingement Heat Transfer: The Influence of Channel Height", 8th International Heat Transfer Conference, San Francisco, pp.1205-1211.

Andrews, G.E. and Hussain, C.I., 1987, "Full Coverage Impingement Heat Transfer: The Influence of Crossflow". AIAA/ASME/SAE/ASEE 23rd Joint Propulsion Conference, AIAA Paper 87-2010.

Andrews, G.E., Asere, A.A., Hussain, C.I. and Mkpadi, M.C., 1985a, "Transpiration and Impingement/Effusion Cooling of Gas Turbine Combustion Chambers". Seventh International Symposium on Air Breathing Engines, Beijing, China, pp.794-803, AIAA/ISABE 85-7095.

Andrews, G.E., Asere, A.A., Gupta, M.L. and Mkpadi, M.C., 1985b, "Full Coverage Discrete Hole Film Cooling: The Influence of Hole Size", ASME Paper 85-GT-53. International Journal of Turbo and Jet Engines, Vol. 2, pp. 213-225.

Andrews, G.E., Gupta, M.L. and Mkpadi, M.C., 1985c, "Full Coverage Discrete Hole Wall Cooling: Cooling Effectiveness", ASME Paper 84-GT-212. Int. J. of Turbo and Jet Engines, Vol. 2, p.199-212.

Andrews, G.E., Asere, A.A., Hussain, C.I. and Mkpadi, M.C., 1985d, "Full Coverage Impingement Heat Transfer: The Variation in Pitch to Diameter Ratio at a Constant Gap", AGARD CP-390, Paper no. 26, 13pp., Propulsion and Energetic Panel, 65th Symposium, 'Heat Transfer and Cooling in Gas Turbines', Bergen, Norway.

Andrews, G.E., Alikhanizadeh, M., Asere, A.A., Hussain, C.I., Koshkbar Azari, M.S. and Mkpadi, M.C., 1986a, "Small Diameter Film Cooling Holes: Wall Convective Heat Transfer", ASME Paper 86-GT-225, Trans-ASME, J. Turbo-machinery, Vol. 108, pp.283-289.

Andrews, G.E., Alikhanizadeh, M., Bazdidi-Tehrani, F., Hussain, C.I. and Koshkbar Azari, M.S., 1987a, "Small Diameter Film Cooling Holes: The Influence of Hole Size and Pitch", ASME/AIChE Heat Transfer Conference, ASME Paper 87-HT-28.

Andrews, G.E., Durance, J., Hussain, C.I. and Ojobor, S.N., 1987b, "Full Coverage Impingement Heat Transfer: The Influence of the Number of Holes", ASME Paper 87-GT-93, Trans. ASME, J. Turbo-machinery, Vol. 109, pp.557-563.

Andrews, G.E., Asere, A.A., Hussain, C.I., Mkpadi, M.C. and Nazari, A., 1988, "Impingement/Effusion Cooling: Overall Wall Heat Transfer", ASME Paper 88-GT-290.

Chance, J.L., 1974, "Experimental Investigations of Air Impingement Heat Transfer Under an Array of Round Jets", Tappi, Vol. 57, pp.108-112.

Creare, 1985, "Fluent Manual: Version 2.8", Creare Incorporated, TN-369 Rev. 2.

Florschuetz, L.W., Truman, C.R. and Metzger, D.E., "Steamwise Flow and Heat Transfer Distribution for Jet Array Impingement with Initial Crossflow", Trans. ASME, J. Heat Transfer, Vol. 103, pp. 337-342.

Hollworth, B.R. and Berry, R.D., 1978, "Heat Transfer for Arrays of Impinging Jets with Large Jet-to-Jet Spacing", ASME Paper 78-GT-117.

Hollworth, B.R. and Dagan, L., 1980, "Arrays of Impinging Jets with Spent Fluid Removal Through Vent Holes on the Target Surface. Part 1: Average Heat Transfer", Trans. ASME, J.Eng. Power, Vol. 102, pp.994-999.

Hollworth, B.R., Lehmann, G. and Rosiczkowski, J., 1981, "Arrays of Impinging Jets with Spent Fluid Removal Through Vent Holes on the Target Surface. Part 2: Local Heat Transfer", ASME Paper 81-HT-76.

Kercher, D.M. and Tabakoff, W., 1970, "Heat Transfer by a Square Array of Round Air Jets Impinging Perpendicular to a Flat Surface", Trans. ASME, J. Eng. Power, pp. 73-82.

Tabakoff, W. and Clevenger, W., 1972, "Gas Turbine Blade Heat Transfer Augmentation by Impingement of Air Jets having Various Configurations", Trans. ASME, J. Eng. Power, pp.51-60.